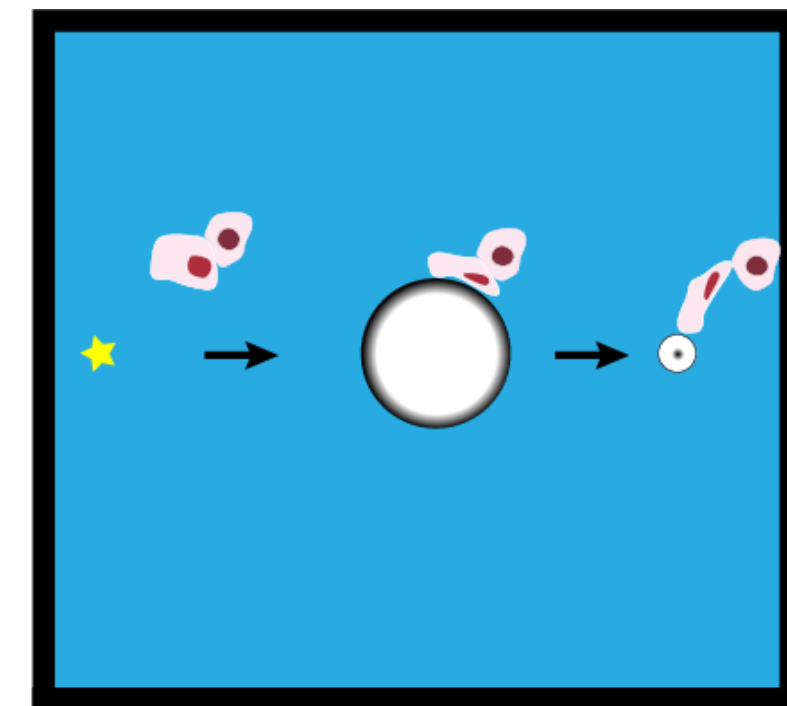


Gregory J. Anthony, Viktor Bollen, Steffen Sammet, Kenneth B. Bader

Department of Radiology, University of Chicago, Chicago, IL, USA

## Introduction and Purpose

- Histotripsy liquefies tissue via mechanical action of bubble clouds
  - Treatment of liver, kidney, prostate, thrombosis<sup>1</sup>
- Multi-modal image guidance could improve clinical translation and treatment outcomes
  - Diagnostic ultrasound imaging visualizes bubble cloud activity<sup>2,3</sup>
  - MRI visualizes changes in tissue structure<sup>4</sup>

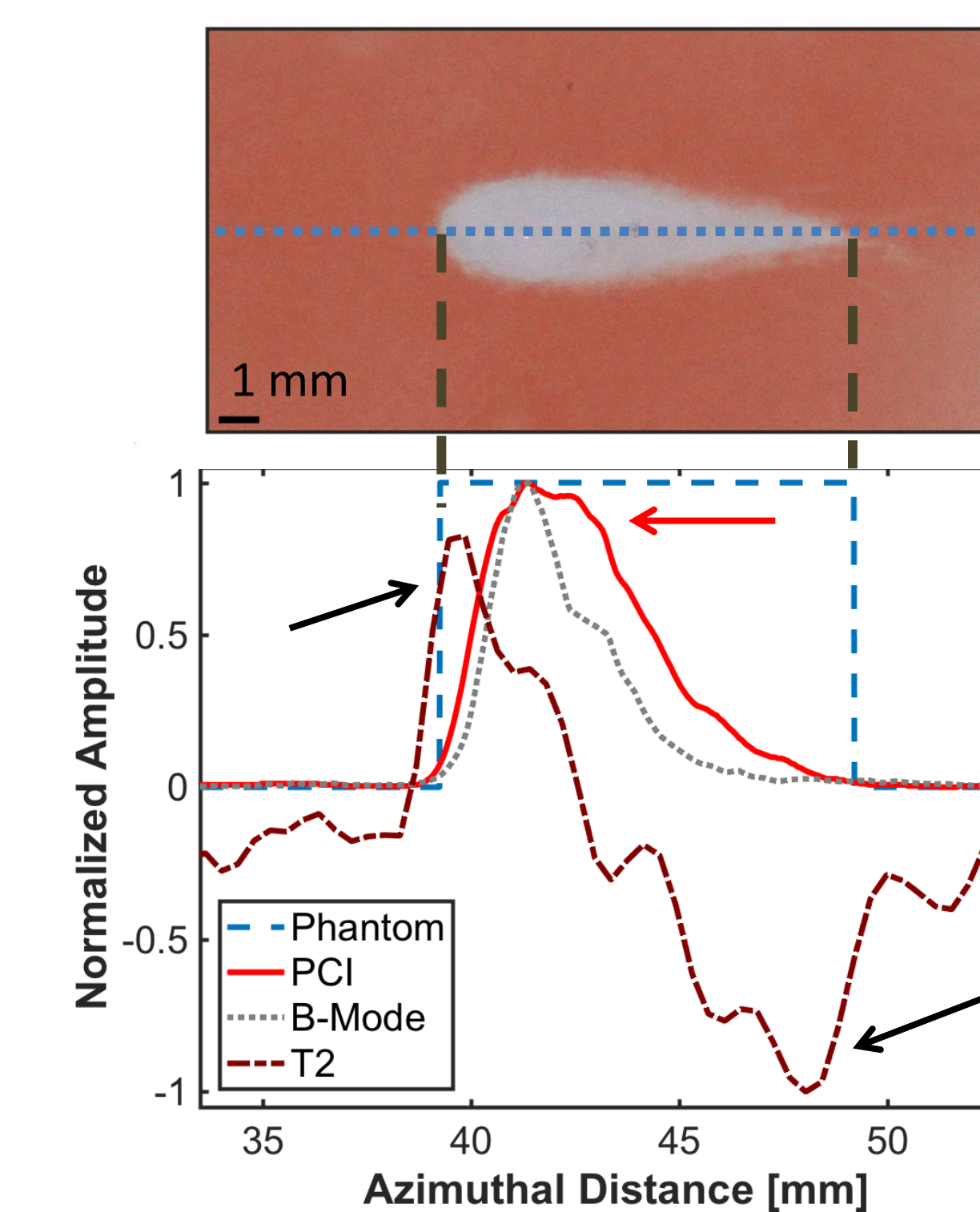


Legend: Cavitation Nucleus, Active Bubble, Target Cells. Illustration of bubble activity inducing strain and damage to nearby cells<sup>5</sup>

## Results

- Phantom liquefaction, high PCI power and B-mode grayscale, and changes in MR parameters correlated well spatially
- $T_1$  increased in the liquefaction zone, and  $T_2$  exhibited spatially varying changes
- Largest changes in  $T_2$  corresponded to areas of low PCI/B-mode grayscale intensity
- $T_2$ W and gross imaging indicated changes in structure of the liquefaction zone as peak negative pressure increased
- Areas under the ROC curve (AUCs) were significantly greater than 0.5, indicating improved prediction of liquefaction locations over guessing for all imaging modalities

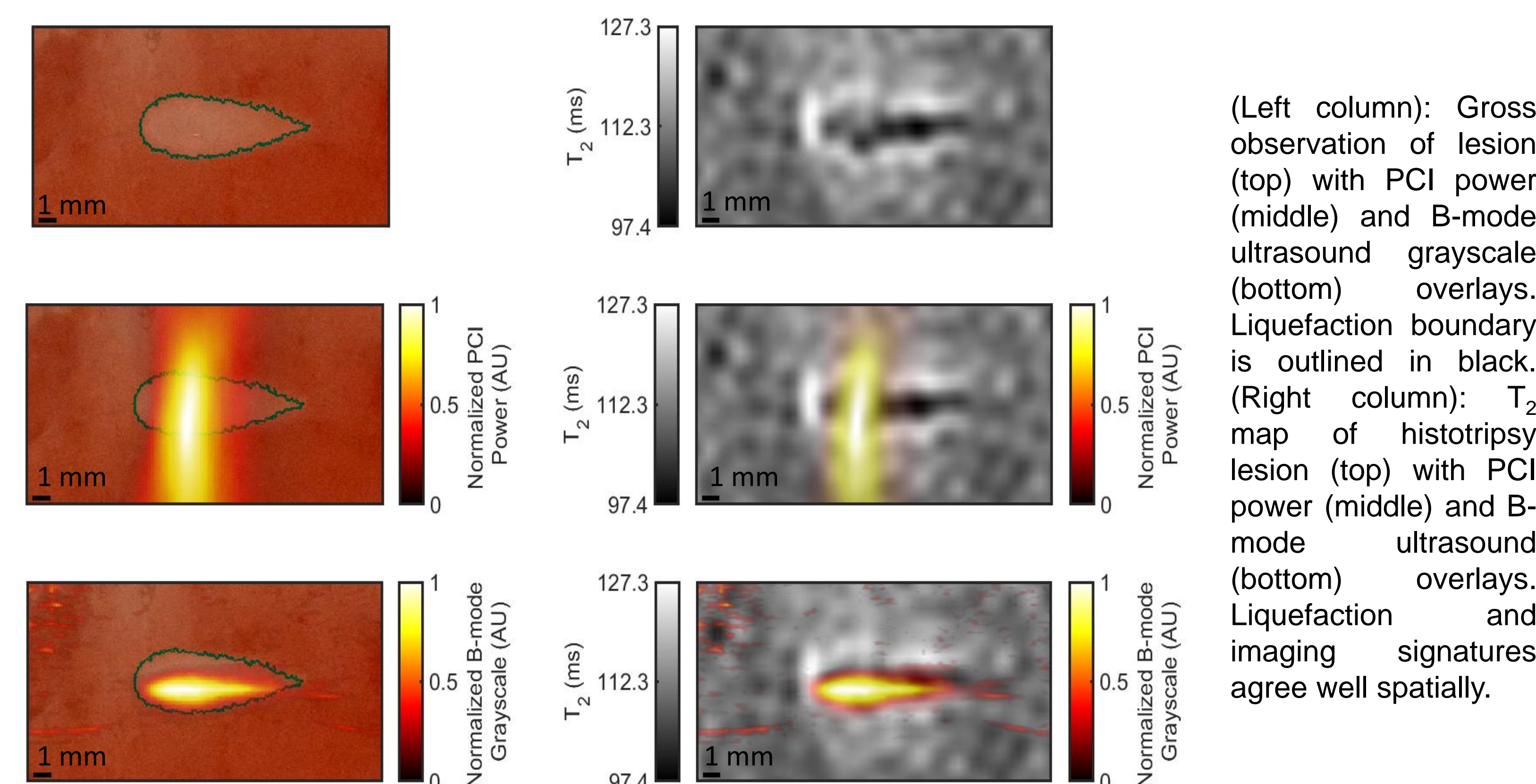
## Results (cont.)



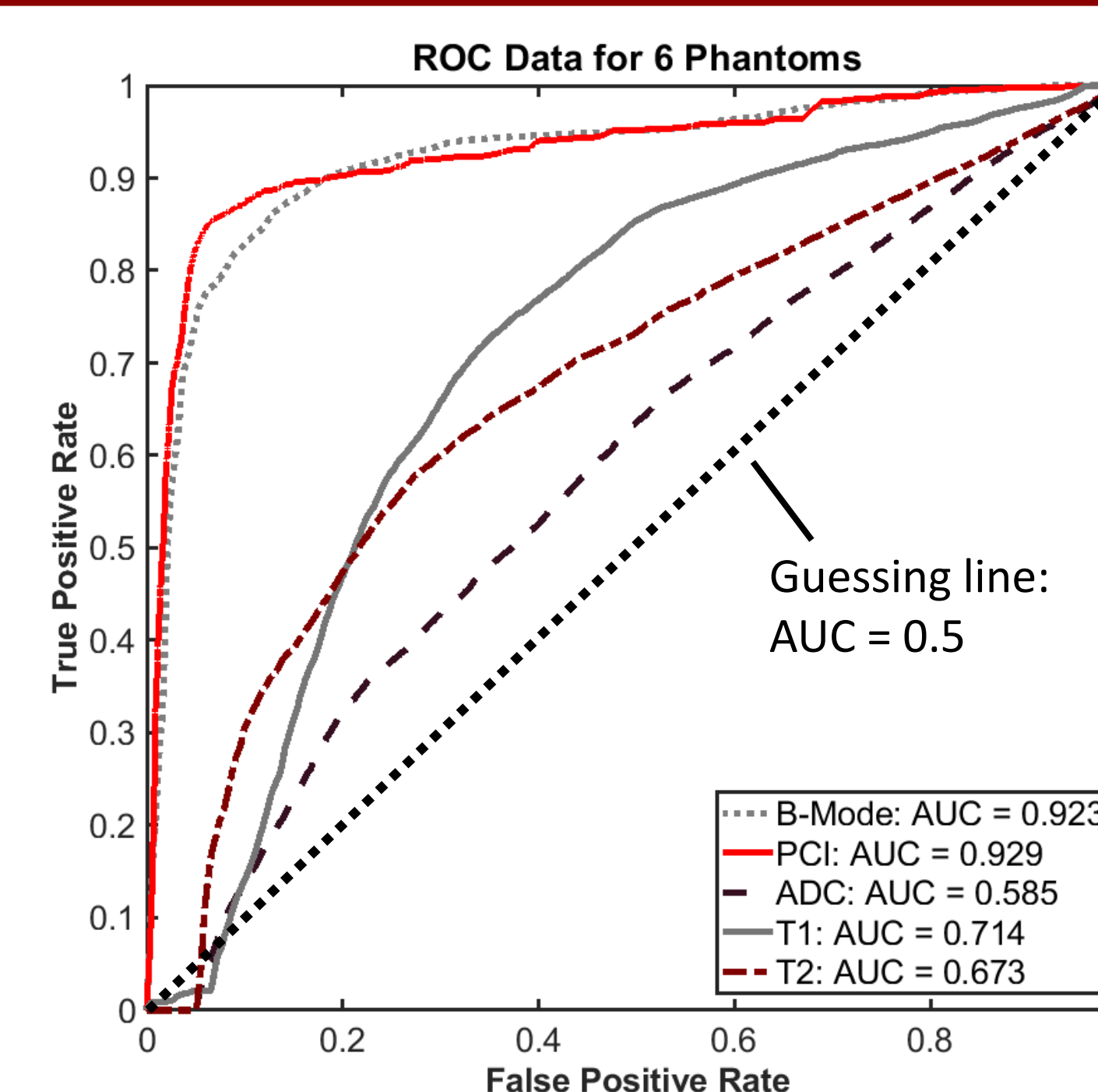
Profile along a histotripsy lesion's azimuthal dimension, plotting presence of liquefaction (blue dotted line) against normalized PCI power (red solid line), B-mode ultrasound grayscale value (gray dotted line), and normalized change in  $T_2$  from background value (brown dash-dot line). The areas of greatest change in  $T_2$  (black arrows) correspond to areas of low PCI power and B-mode grayscale value (red arrow) within the lesion.

## Materials and Methods

- Construct agarose phantoms with 15% v/v porcine red blood cell layers<sup>6</sup>
- Initiate 1 MHz histotripsy insonations of 13 – 25 MPa peak negative pressure, 100 Hz pulse repetition frequency, 5 cycle pulse duration
- Acquire B-mode ultrasound and passive cavitation imaging (PCI)<sup>7</sup> data during insonation
- Acquire 3T MR  $T_1$ - and  $T_2$ W images, and  $T_1$ ,  $T_2$ , and ADC maps
- Section phantoms and register liquefaction zones with diagnostic ultrasound/MR images
- Assess prediction of liquefaction from diagnostic ultrasound imaging or MRI via ROC analysis



(Left column): Gross observation of lesion (top) with PCI power (middle) and B-mode ultrasound grayscale (bottom) overlays. Liquefaction boundary is outlined in black. (Right column):  $T_2$  map of histotripsy lesion (top) with PCI power (middle) and B-mode ultrasound (bottom) overlays. Liquefaction and imaging signatures agree well spatially.



ROC curves obtained using PCI power (red solid line), B-mode grayscale (gray dotted line), ADC (black dashed line),  $T_1$  (gray solid line), and  $T_2$  (brown dash-dot line) to predict presence of liquefaction along azimuth dimension of histotripsy lesions in six phantoms. The black dotted line indicates the resulting ROC curve from guessing liquefaction or not liquefaction. The area under the curve (AUC) indicates the quality of a parameter's predictive value.

## Conclusions

- Ultrasound and MR imaging supply complimentary information regarding histotripsy liquefaction
- Multi-modal imaging with diagnostic ultrasound and MRI may improve assessment of histotripsy treatment zones
- This *in vitro* study is limited in its approximation of actual tissue liquefaction, and the results presented should be validated with *in vivo* studies

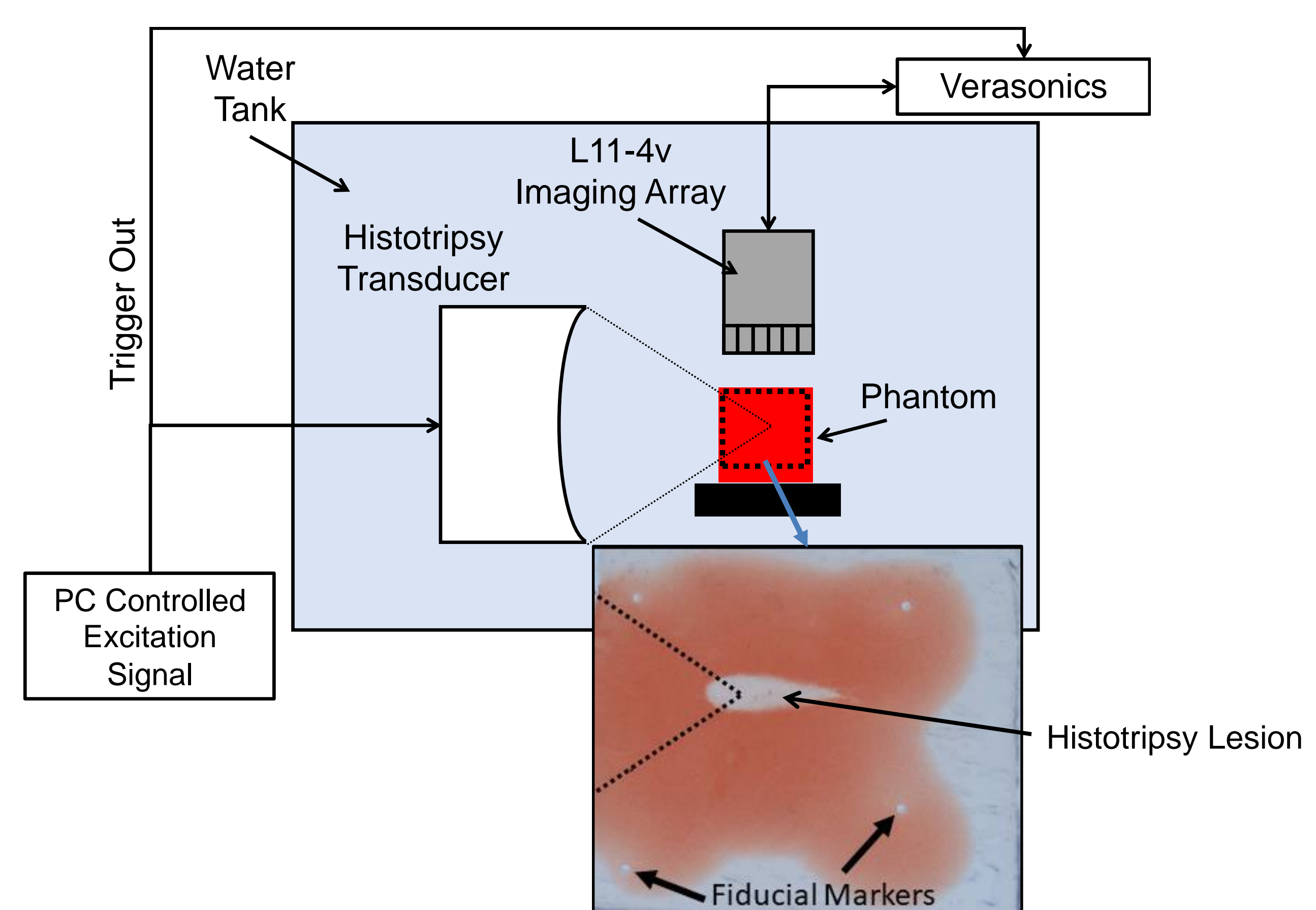
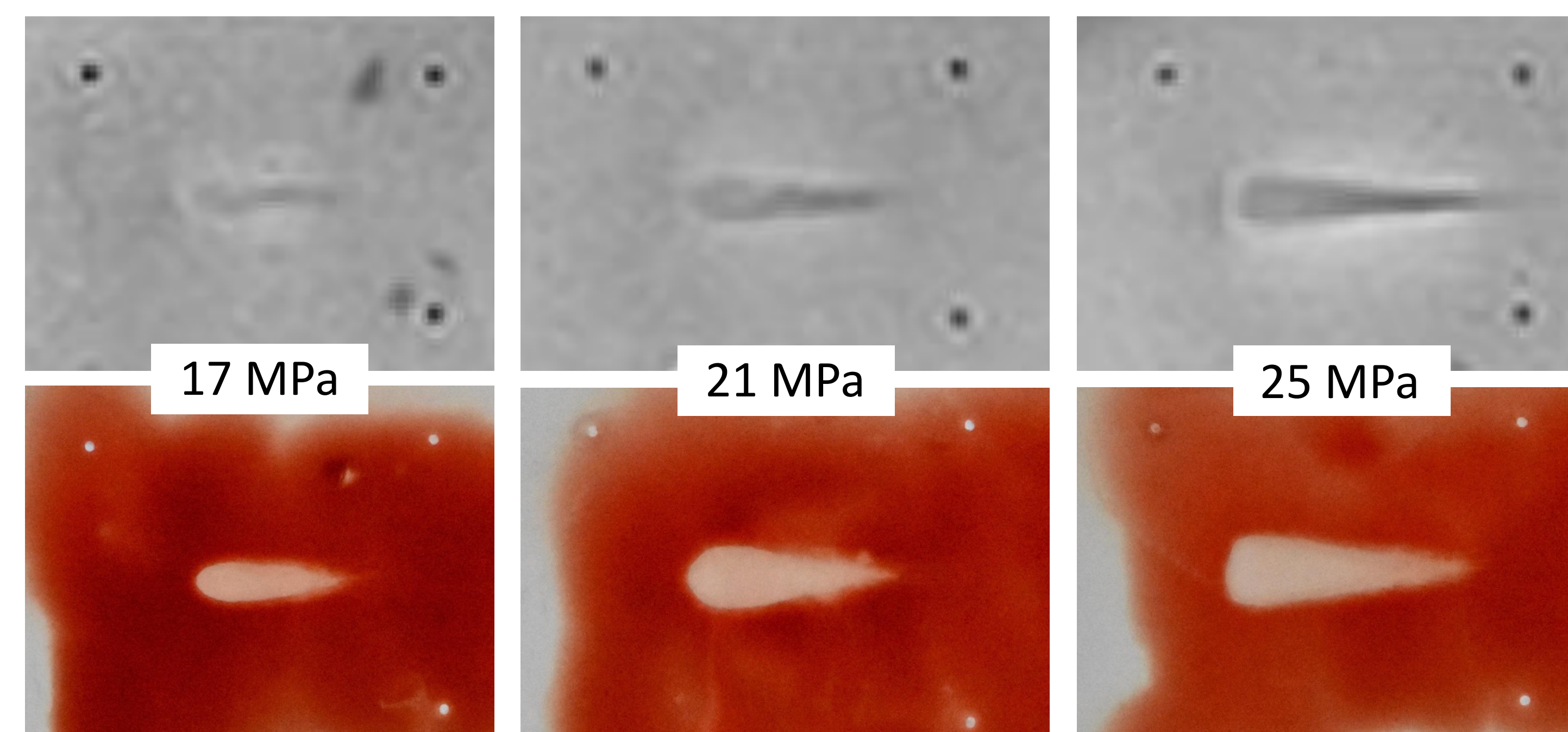


Diagram of experimental setup. Histotripsy pulses are initiated in an agarose phantom while PCI and B-mode ultrasound data are acquired.



$T_2$ W images (top row) and gross observations (bottom row) of histotripsy lesions generated with 17 (left), 21 (middle), and 25 (right) MPa PNP. As pressure increases, the lesion is more sharply delineated by  $T_2$ W MRI, a stronger hypointense signal is seen at the distal (right) end, and the proximal (left) end of the lesion flattens out.

## References

- Khokhlova et al., *Clin Oncol*, **23** (2): 117–127, 2011.
- Bader et al., *IEEE Trans Med Imaging*, **37** (1): 106–115, 2018.
- Bader, *J Acoust Soc Am*, **140** (4): 3084, 2016
- Allen et al., *Phys Med Biol*, **62** (17): 7167, 2017.
- Bader et al., *Ultrasound Med Biol* (under review).
- Maxwell et al., *Ultrasound Med Biol*, **36** (12): 2132–2143, 2010.
- Haworth et al., *IEEE Trans Ultrason Ferroelectr Freq Control*, **64** (1): 177–191, 2017.

## Acknowledgements

Funding provided by the NIH (Grants K12CA139160 and R01HL13334), Cancer Research Foundation, and the University of Chicago Comprehensive Cancer Center.